voltammogram of L_2Fe^{III} in CH_2Cl_2 (0.1 M $[(n\text{-butyl})_4N]PF_6$) at a glassy-carbon working electrode shows one quasi-reversible one-electron-transfer wave ($E_{1/2}$ = −1.86 V vs Fc^+/Fc) in the potential range +0.3 to −1.8 V vs Ag/AgCl, which is assigned to the couple $L^2Fe^{III}/[L^2Fe^{II}]^-$. This negative redox potential is in good agreement with other (phenolate)- or (catecholate)iron(III) complexes, e.g. $[Fe(salen)PD]^{-/2-}$ (−1.87 V vs Fc^+/Fc) and $[Fe(salen)DBcat]^{-/2-}$ (−2.0 V vs Fc^+/Fc).[21] It indicates the enormous stabilization of the ferric phenolate over the ferrous phenolate species.

The cyclic voltammogram of L^2Mn^{III} in CH_2Cl_2 (0.1 M $[(n\text{-butyl})_4N]PF_6$) is shown in Figure 7. Two reversible one-electron-transfer waves are detected in the potential range 0.8 V to −0.9 V vs Ag/AgCl at $E^1_{1/2}$ = −0.45 V and $E^2_{1/2}$ = −0.982 V vs Fc^+/Fc. The first process corresponds to the Mn(IV)/Mn(III) couple, and the second, to the Mn(III)/Mn(II) couple. The reversibility of the latter process is impaired at slower scan rates (<200 mV s^{-1}) due to the lability of the reduced Mn(II) form. Similar redox chemistry has been reported for a series of manganese complexes containing a Schiff base ligand derived from substituted salicylaldehydes.[22]

Due to severe absorption effects of L^2Co^{III} in CH_3CN or CH_2Cl_2 at the surface of the working electrode (glassy-carbon or Pt-button), it has not been possible to obtain a reproducible cyclic voltammogram of this species.

Acknowledgment. We thank the Fonds der Chemischen Industrie for financial support.

Supplementary Material Available: For complexes **1** and **2**, listings of positional parameters, thermal parameters, crystallographic data (Table S1), calculated positions of hydrogen atoms, and bond lengths and bond angles (11 pages); listings of observed and calculated structure factors (36 pages). Ordering information is given on any current masthead page.

(21) Heistand, R. H., II; Lauffer, R. B.; Fikrig, E.; Que, L., Jr. *J. Am. Chem. Soc.* **1982**, *104*, 2789.

(22) Coleman, W. M.; Bogges, R. K.; Hughes, J. W.; Taylor, L. T. *Inorg. Chem.* **1981**, *20*, 1253.

Contribution from the Departments of Chemistry, Southwest Texas State University, San Marcos, Texas 78666, University of Texas at Austin, Austin, Texas 78712, and University of Michigan, Ann Arbor, Michigan 48109-1055

Monomeric and Dimeric Vanadium(IV) and -(V) Complexes of *N*-(Hydroxyalkyl)salicylideneamines: Structures, Magnetochemistry, and Reactivity

Carl J. Carrano,*[,†] Christine M. Nunn,[‡] Roger Quan,[§] Joseph A. Bonadies,[§,∥] and Vincent L. Pecoraro*[,§]

Received June 28, 1989

The *N*-(hydroxyalkyl)salicylideneamine ligands (H_2SALAHE = 2-(salicylideneamino)-1-hydroxyethane; H_2SALAHP = 3-(salicylideneamino)-1-hydroxypropane; H_2SALAMHP = 2-(salicylideneamino)-2-methyl-1-hydroxypropane; H_2SALAMHE = 2-(salicylideneamino)-2-methyl-1-hydroxyethane [or 2-(salicylideneamino)-1-hydroxypropane]; H_2SALATHM = tris(hydroxymethyl)(salicylideneamino)methane) form monomeric and dimeric complexes when reacted with VO^{2+} salts in organic solvents. When a 2:1 ligand to metal ratio is used in the synthesis, the mononuclear $VO(HSALAHE)_2$ (**1**) crystallizes as a dark green solid with X-ray diffraction analysis demonstrating it to be a five-coordinate species with the ligands bound in a bidentate fashion by using the phenolate and imine nitrogen atoms. When a 1:1 ligand to metal ratio is used and the reaction maintained strictly anaerobic, a dimer of composition $[VO(SALAHE)]_2$ (**3**) is recovered. X-ray crystallography demonstrates that the ligand is a tridentate dianion in this complex, which is a dialkoxy-bridged dimer with a syn orientation of vanadyl oxygen atoms. This structure is in contrast to a polymeric material of the same composition $[VO(SALAHE)]_n$ (**2**), which is thought to be an infinite spin ladder. Magnetic exchange in **2** (1.01 μ_B/V) is slightly greater than in **3** (1.52 μ_B/V), which probably reflects the larger extent of σ overlap between d_{xy} orbitals of the two vanadium atoms in the planar **2** as opposed to the bent **3**. These vanadium(IV) dimers can be converted to an unusual V(V) dimer of composition $[V^VOL]_2O$. An X-ray diffraction analysis of the SALAMHP derivative **4c** shows that the ligands are again tridentate; however, one alkoxide acts as a weak bridge while the other is nonbridging. The strongest link between the vanadium atoms is a nonlinear oxo group that is part of the $V_2O_3^{4+}$ core. Crystallographic parameters for **1**, **3**, and **4c** are as follows. $VO(SALAHE)_2$ (**1**) ($C_{18}H_{20}N_2O_5V$): MW, 395.31; *a*, 10.301 (2) Å; *b*, 8.733 (3) Å; *c*, 20.575 (5) Å; β, 104.19 (2)°; *V*, 1794.4 (6) Å^3; monoclinic ($P2_1/c$); *Z* = 4; for 2953 unique data ($3 < 2\theta < 48°$) and 2010 data with $I > 2\sigma(I)$, the structure refined to $R(F_o)$ = 0.062. $[VO(SALAHE)]_2$ (**3**) ($C_{18}H_{18}N_2O_6V_2$): MW, 460; *a*, 22.530 (3) Å; 6.530 (6) Å; *c*, 13.115 (15) Å; β, 93.04 (10)°; *V*, 1927 (4) Å^3; monoclinic ($P2_1/c$); *Z* = 4; for 2510 unique data ($0 < 2\theta < 45°$) and 1387 data with $I > 2\sigma(I)$, the structure refined to $R(F_o)$ = 0.077. $[VO(SALAMHP)]_2O$ (**4c**) ($C_{22}H_{26}N_2O_7V_2$): MW, 532.4; *a*, 33.929 (6) Å; *b*, 7.203 (2) Å; *c*, 19.618 (5) Å; β, 98.97 (2)°; *V*, 4736.1 (8) Å^3; monoclinic ($C2/c$); *Z* = 8; for 4248 unique data ($3 < 2\theta < 50°$) and 2662 data with $I > 3\sigma(I)$, the structure refined to $R(F_o)$ = 0.052.

Introduction

Vanadium is receiving considerable attention as a biologically important metal due to the recent discovery of the first two vanadoenzymes (bromoperoxidase from marine algae[1,2] and nitrogenase from *Azotobacter vinelandii*[3]). The nitrogenase most likely contains a modified form of the FeMo cofactor in which vanadium replaces molybdenum.[4-6] Much less is known about metal ligation in the bromoperoxidase.[7-12] It has been established that the catalytically active form of the enzyme contains a mononuclear V(V) center and that neither a metal sulfide cluster nor a vanadoporphyrin is an appropriate description of the active site. Presumably amino acid residues such as aspartate, glutamate, serine, threonine, tyrosine, and histidine supply the majority of heteroatom donors, although one or two terminal oxo groups are probably present.

† Southwest Texas State University.
‡ University of Texas at Austin.
§ University of Michigan.
∥ Present address: Dow Chemical, USA, Midland, MI.

(1) Vilter, H. *Phytochemistry* **1984**, *23*, 1387.
(2) de Boer, E.; van Kooyk, Y.; Tromp, M. G. M.; Plat, H.; Wever, R. *Biochim. Biophys. Acta* **1986**, *869*, 48.
(3) Robson, R. L.; Eady, R. R.; Richardson, T. H.; Miller, R. W.; Hawkins, M.; Postgate, J. R. *Nature (London)* **1986**, *322*, 388.
(4) Kovacs, J. A.; Holm, R. H. *Inorg. Chem.* **1987**, *26*, 702.
(5) Kovacs, J. A.; Holm, R. H. *Inorg. Chem.* **1987**, *26*, 711.
(6) Morningstar, J. E.; Johnson, M. K.; Case, E. E.; Hales, B. J. *Biochemistry* **1987**, *26*, 1795.
(7) de Boer, E.; Tromp, M. G. M.; Plat, H.; Krenn, B. E.; Wever, R. *Biochim. Biophys. Acta* **1986**, *872*, 104.
(8) de Boer, E.; Wever, R. *Recl. Trav. Chim. Pays-Bas* **1987**, *106*, 409.
(9) de Boer, E.; Boon, K.; Wever, R. *Biochemistry* **1988**, *27*, 1629.
(10) de Boer, E.; Wever, R. *J. Biol. Chem.* **1988**, *263*, 12326.
(11) Wever, R.; Krenn, B. E.; de Boer, E.; Offenberg, H.; Plat, H. In *Oxidases and Related Redox Systems*; King, T. E., Mason, H. S., Morrison, M., Eds.; Alan R. Liss Publishers: New York, 1988; p 477.
(12) Everett, R. R.; Butler, A. *Inorg. Chem.* **1989**, *28*, 393.

0020-1669/90/1329-0944$02.50/0

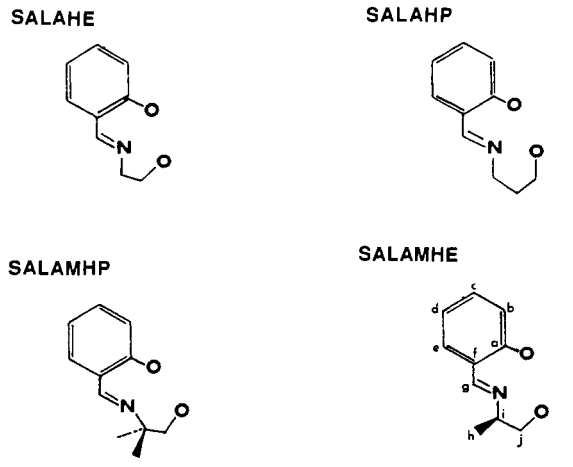

Figure 1. Salicylideneamine ligands as dianions used in this study. Abbreviations are explained in ref 39. Letters correspond to carbon positions for ^{13}C NMR spectra.

In order to understand how vanadium might function in a complex biomolecule, it is first necessary to define its basic coordination chemistry with biologically relevant ligands. Work with model complexes to mimic the phenolate oxygen of tyrosine and the imidazole nitrogen of histidine have already lead to interesting results.[13-30] In this report, we describe our initial efforts to explore alkoxide coordination such as might result from deprotonated serine or threonine residues. The systems we have chosen to examine first are the *N*-(hydroxyalkyl)salicylideneamines. Vanadium(IV) complexes of these ligands have been reported a number of times,[31-37] but considerable controversy still surrounds their formulation and magnetic properties. We have observed that a wide range of dimers in the +4 and +5 oxidation level are easily accessible. Herein, we provide the first X-ray crystallographic structural information for the V(IV) dialkoxy-bridged dimers, which serves to clarify the previously disparate magnetochemistry and also provides structural characterization of a rare example of $(V_2O_3)^{4+}$ core with a non-linear bridging oxo group.

Experimental Section

Vanadyl acetylacetonate was prepared as previously described.[38] Ammonium vanadate and vanadyl sulfate were obtained from Aldrich Chemicals and used as received. Solvents were dried with the appropriate reagents and distilled under Ar or N_2. Syntheses of V(IV) complexes were performed under Ar or N_2 by using standard Schlenk techniques unless otherwise stated. All the V(IV) complexes isolated thus far undergo air oxidation in solution to V(V) species. This oxidation is relatively slow in good donor solvents such as DMF, but is rapid in methylene chloride. Thus, deliberate synthesis of vanadium(V) complexes were carried out in air using V(IV) starting materials and CH_2Cl_2 as a solvent.

***N*-(Hydroxyalkyl)salicylideneamine Ligands (SALA Series[39]).** The hydroxyl-rich Schiff base ligands used in this study (Figure 1) were prepared by refluxing equimolar quantities of the appropriate alkanolamine with salicylaldehyde in methanol for 30 min. In some cases, the methanol was removed by rotary evaporation to yield a deep yellow oil that crystallized on standing. NMR and IR spectral data indicated that the products contained only a trace of unreacted material and, therefore, were used without further purification. One could also react the vanadium salt of choice directly in the reaction mixture used to prepare the ligand (template reaction) and recover the identical vanadium complexes without affecting the overall yield.

$VO(HSALAHE)_2$ (1). $VO(acac)_2$ (1.2 g, 4.5 mmol) was added with stirring to 1.5 g of $H_2SALAHE$ (9.1 mmol) dissolved in dry methanol, giving a deep green solution. The volume was reduced to half and the reaction allowed to stand at −20 °C for 2 days after which a dark green crystalline mass was filtered off, washed with ether, and dried. Anal. Calcd for $C_{18}H_{20}N_2O_5V$: C, 54.68; H, 5.06; N, 7.09. Found: C, 54.74; H, 5.00; N, 7.01.

$[VO(SALAHE)]_x$ (2). $VOSO_4$ (1.6 g, 10 mmol) was dissolved in 50 mL of H_2O and then added to 1.6 g of $H_2SALAHE$ (10 mmol) dissolved in 50 mL of methanol. Stirring in air for 30 min gave a green solution with a green-gray precipitate. The precipitate was filtered off, washed with water and methanol, and air-dried. Yield: 0.67 g (30%). Anal. Calcd for $C_9H_9NO_3V$: C, 46.96; H, 3.91; N, 6.09. Found: C, 46.7; H, 4.09, N, 5.94. The related $SALAHP^{2-}$, $SALAMHP^{2-}$, and $SALAHME^{2-}$ complexes were prepared in an analogous manner.

$[VO(SALAHE)]_2$ (3). If a 1:1 molar ratio of $H_2SALAHE$ to $VO(acac)_2$ is reacted as above for **2** except that it is kept under strictly anaerobic conditions, a red complex with an analytical composition similar to **2** can be isolated. Filtration of the reaction mixture under N_2 gave a small quantity of red crystals, **3** (yield 20%). Anal. Calcd for $C_{18}H_{18}N_2O_6V_2$: C, 46.96; H, 3.91; N, 6.09; V, 22.17. Found: C, 47.15; H, 4.00; N, 6.00; V, 21.66.

$\{[VO(SALAHE)]_2O\}$ (4a). $VO(acac)_2$ solid (1.34 g, 5 mmol) was added to 1.63 g of $H_2SALAHE$ (10 mmol) dissolved in 200 mL of methylene chloride and the mixture stirred in air. A green-gray precipitate formed initially but redissolved to yield a deep red-brown solution after 2 days. Allowing the solution to stand yielded a crop of deep red-brown needles, which were filtered, washed with ether, and air-dried. Yield: 0.9 g, 73%. Evaporation of the methylene chloride followed by recrystallization of the residue from hot acetonitrile gave a further yield of product. Anal. Calcd for $C_{18}H_{18}N_2O_7V_2 \cdot {}^1/_2H_2O$, C, 44.54; H, 3.92; N, 5.77. Found: C, 44.33; H, 3.62; N, 5.69. The related $SALAHP^{2-}$ (**4b**), $SALAMHP^{2-}$ (**4c**), and $SALAMHE^{2-}$ (**4d**) complexes were prepared in an analogous manner. The deep red-brown solutions in methylene chloride were taken to dryness and the residues recrystallized from hot acetonitrile. All compounds gave satisfactory elemental analyses.

Collection and Reduction of X-ray Data. Large crystals of **1**, **3**, and **4c** were grown as described above. If needed, the crystals were cut with a razor blade and mounted in Lindeman capillaries. Crystals of **4a** were of two habits when recrystallized from acetonitrile: thin red needles and short rectangular blocks. The blocks were picked from solution by visual inspection and mounted. Crystals of **4c** appeared only in the blocklike habit, and several of these were also mounted in Lindeman capillaries as previously described. A better data set was collected for **4c**, and its solution was carried to completion. The preliminary structure solution for **4a** indicated that it was isostructural with **4c** and thus was not carried further.

Crystals were transferred to either a Enraf-Nonius CAD4 (University of Texas at Austin) or Syntex $P2_1$ (University of Michigan) diffractom-

(13) Li, X.; Lah, M. S.; Pecoraro, V. L. *Inorg. Chem.* **1988**, *27*, 4567.
(14) Scheidt, W. R.; Collins, D. M.; Hoard, J. L. *J. Am. Chem. Soc.* **1971**, *93*, 3873.
(15) Scheidt, W. R.; Countryman, R.; Hoard, J. L. *J. Am. Chem. Soc.* **1971**, 93, 3878.
(16) Scheidt, W. R. *Inorg. Chem.* **1973**, *12*, 1758.
(17) Giacomelli, A.; Floriani, C.; de Souza Duarte, A. O.; Chiesi-Villa, A.; Guastini, C. *Inorg. Chem.* **1982**, *21*, 3310.
(18) Wieghardt, K.; Bossek, U.; Volckmar, K.; Swirdoff, W.; Weiss, J. *Inorg. Chem.* **1984**, *23*, 1387.
(19) Djordjevic, C.; Lee, M.; Sinn, E. *Inorg. Chem.* **1989**, *28*, 719.
(20) Stomberg, R.; Olson, S.; Svenson, I.-B. *Acta Chem. Scand.* **1984**, *A38*, 653.
(21) Szentivanyi, H.; Stomberg, R. *Acta Chem. Scand.* **1983**, *A37*, 553.
(22) Stomberg, R.; Olson, S. *Acta Chem. Scand.* **1984**, *A38*, 801.
(23) Launay, J.-P.; Jeannin, Y.; Daoudi, M. *Inorg. Chem.* **1985**, *24*, 1052.
(24) Babonneau, F.; Sanchez, C.; Livage, J.; Launay, J. P.; Daoudi, M.; Jeannin, Y. *Nouv. J. Chim.* **1982**, *6*, 353.
(25) Nishizawa, M.; Hirotsu, K.; Ooi, S.; Saito, K. *J. Chem. Soc., Chem. Commun.* **1979**, 707.
(26) Kojima, A.; Okazaki, K.; Ooi, S.; Saito, K. *Inorg. Chem.* **1983**, *22*, 1168.
(27) Bonadies, J. A.; Pecoraro, V. L.; Carrano, C. J. *J. Chem. Soc., Chem. Commun.* **1986**, 1218.
(28) Bonadies, J. A.; Butler, W. M.; Pecoraro, V. L.; Carrano, C. J. *Inorg. Chem.* **1987**, *26*, 1218.
(29) Pecoraro, V. L.; Bonadies, J. A.; Marese, C. A.; Carrano, C. J. *J. Am. Chem. Soc.* **1985**, *107*, 1651.
(30) Bonadies, J. A.; Carrano, C. J. *J. Am. Chem. Soc.* **1986**, *108*, 4088.
(31) Kuge, Y.; Yamada, S. *Bull. Chem. Soc. Jpn.* **1970**, *43*, 3972.
(32) Poddar, S. N.; Dey, K.; Hadler, J.; Nathsarkar, S. C. *J. Indian Chem. Soc.* **1970**, *47*, 43.
(33) Syamal, A.; Carrey, E. F.; Theriot, L. J. *Inorg. Chem.* **1973**, *12*, 245.
(34) Syamal, A.; Kale, K. S. *Indian J. Chem.* **1977**, *15A*, 431.
(35) Syamal, A. *Indian J. Chem.* **1973**, *11*, 363.
(36) Rao, G. N.; Rustagi, S. C. *Indian J. Chem.* **1973**, *11*, 1181.
(37) Yamada, S.; Kuge, Y. *Synth. React. Inorg. Met.-Org. Chem.* **1986**, *16* (3), 397.
(38) Ferndius, W. C.; Byant, B. E. *Inorg. Synth.* **1957**, *5*, 114.
(39) Abbreviations used: $H_2SALAHE$ = 2-(salicylideneamino)-1-hydroxyethane; $H_2SALAHP$ = 3-(salicyclideneamino)-1-hydroxypropane; $H_2SALAMHP$ = 2-(salicylideneamino)-2-methyl-1-hydroxypropane; $H_2SALAMHE$ = 2-(salicylideneamino)-2-methyl-1-hydroxyethane [or 2-(salicylideneamino)-1-hydroxypropane]; $H_2SALATHM$ = tris(hydroxymethyl)(salicylideneamino)methane; acac = monoanion of 2,4-pentanedione.

Table I. Crystallographic Data for **1**, **3**, and **4c**

Complex **1**	
$C_{18}H_{20}N_2O_5V$	$P2_1/c$ No. 14
fw = 395.31	T = 24 °C
a = 10.301 (2) Å	λ = 0.7107 Å
b = 8.733 (3) Å	ρ_{calcd} = 1.463 g cm^{-3}
c = 20.575 (5) Å	μ = 5.6 cm^{-1}
β = 104.19 (2)°	$R(F_o)$ = 0.062
V = 1794.4 (8) Å^3	$R_w(F_o)$ = 0.071
Z = 4	
Complex **3**	
$C_{18}H_{18}N_2O_6V_2$	$P2_1/c$ No. 14
fw = 460	T = 25 °C
a = 22.530 (3) Å	λ = 0.7107 Å
b = 6.530 (6) Å	ρ_{calcd} = 1.586 g cm^{-3}
c = 13.115 (15) Å	μ = 9.5 cm^{-1}
β = 93.04 (10)°	$R(F_o)$ = 0.077
V = 1927 (4) Å^3	$R_w(F_o)$ = 0.076
Z = 4	
Complex **4c**	
$C_{22}H_{26}N_2O_7V_2$	$C2/c$ No. 15
fw = 532.4	T = 24 °C
a = 33.929 (6) Å	λ = 0.7107 Å
b = 7.203 (2) Å	ρ_{calcd} = 1.493 g cm^{-3}
c = 19.618 (5) Å	μ = 8.1 cm^{-1}
β = 98.97 (2)°	$R(F_o)$ = 0.052
V = 4736.1 (8) Å^3	$R_w(F_o)$ = 0.075
Z = 8	

eter for data collection. Enraf-Nonius CAD4: Preliminary diffractometer data and axial photographs lead to unit cell choices. Following the accurate centering of 24 relatively high angle reflections, intensity data was collected at room temperature by using θ–2θ scans as previously described.[40] No decay or absorption corrections were deemed necessary and thus were *not* applied. The data were reduced and the models refined by using the SDP suite of programs.[41] Structures were solved by standard Patterson or direct-methods procedures (MULTAN) and refined by full-matrix least-squares techniques as previously described.[40] Syntex $P2_1$: Intensity data were obtained at room temperature by using Mo Kα radiation (0.7107 Å) monochromatized from a graphite crystal whose diffraction vector was parallel to the diffraction vector of the sample. Three standard reflections were measured every 50 reflections. Intensity data were collected by using θ–2θ scans. The data were reduced and the model refined by using the SHELEX76[42] program package. The structures were solved with the SHELEX86[42] program package. Computations were carried out on an Amdahl 5860 computer. Atomic scattering factors used were from ref 43.

Abbreviated crystal data and data collection parameters are summarized in Table I (more complete data can be found in Table 23 of the supplementary material). Hydrogen atoms were located, but not refined, and placed at fixed distances from bonded carbon atoms of 0.95 Å in the final difference map in all three structures. Final R indices are also reported in Table I. Fractional atomic coordinates for **1**, **3**, and **4c** are given in Tables II–IV, respectively. Selected bond distances and angles for these compounds are provided in Tables V–VII.

Electrochemical Measurements. Electrochemical measurements were undertaken at 23 ± 2 °C on a BAS-100 electrochemical analyzer. Cyclic voltammetry was performed with a three-electrode system composed of platinum bead, platinum wire, and saturated calomel (SCE, within a Luggin probe) electrodes as the working, auxilary, and reference electrodes, respectively. Tetrabutylammonium hexafluorophosphate, (TBA)PF_6, was used as the supporting electrolyte at 0.1 M concentration. All potentials are referenced versus the ferrocene/ferrocenium couple employed as an external standard.

Spectroscopic and Magnetic Measurements. UV/vis spectra were recorded either on a Perkin-Elmer 553 or a Lambda 9 UV/vis/near-IR spectrophotometer equipped with a Perkin-Elmer 3600 data station. Infrared spectra were recorded on either a Nicolet 60 SX Fourier transform spectrometer or a Perkin-Elmer 683 infrared spectrophotometer with samples prepared as KBr pellets. Solution EPR spectra were recorded on a Bruker ER200 E-SRC spectrometer equipped with a liquid-nitrogen Dewar and a Varian variable-temperature controller. DPPH (g = 2.0037) was used as an external standard. Room-temperature solid-state magnetic moments were calculated from data obtained on a Johnson-Matthey MSB-1 magnetic susceptibility balance. Solution susceptibilities were calculated from data obtained with either a Bruker 360-MHz or 80-MHz NMR spectrometer by the Evans method.[44,45]

Table II. Fractional Atomic Coordinates of the Non-Hydrogen Atoms for $VO(HSALAHE)_2$ (**1**)

atom	x	y	z	B,[a] Å^2
V1	0.8242 (1)	0.0150 (1)	0.15764 (5)	2.50 (2)
O1	0.2452 (5)	0.3550 (5)	0.3680 (2)	3.8 (1)
O2	0.7039 (5)	0.1499 (5)	0.1859 (2)	3.1 (1)
O3	1.1383 (5)	0.0680 (6)	0.3680 (3)	4.2 (1)
O4	1.0061 (4)	0.0237 (6)	0.1545 (2)	3.6 (1)
O5	0.6786 (6)	0.4413 (6)	0.0227 (3)	4.3 (1)
N1	0.9024 (5)	−0.0339 (6)	0.2603 (3)	2.6 (1)
N2	0.7816 (5)	0.1364 (6)	0.0670 (3)	2.7 (1)
C2	0.8401 (7)	−0.0117 (8)	0.3072 (3)	3.1 (1)
C3	1.0338 (7)	−0.1101 (8)	0.2818 (4)	3.1 (2)
C4	1.1455 (7)	0.0066 (9)	0.3033 (4)	3.7 (2)
C5	0.8660 (7)	0.1774 (8)	0.0323 (3)	2.9 (1)
C6	0.6386 (7)	0.1679 (8)	0.0338 (4)	3.4 (2)
C7	0.6002 (8)	0.3320 (9)	0.0484 (4)	3.8 (2)
C11	0.6556 (7)	0.1531 (8)	0.2401 (3)	2.9 (1)
C12	0.5403 (7)	0.2421 (9)	0.2381 (4)	3.9 (2)
C13	0.4857 (8)	0.244 (1)	0.2944 (4)	4.3 (2)
C14	0.4563 (8)	0.661 (1)	0.1479 (4)	4.3 (2)
C15	0.6601 (8)	0.0776 (9)	0.3557 (4)	3.9 (2)
C16	0.7161 (7)	0.0723 (8)	0.2993 (3)	2.9 (1)
C21	1.0742 (7)	0.0802 (8)	0.1127 (3)	2.9 (1)
C22	1.0102 (7)	0.1588 (8)	0.0535 (3)	3.0 (1)
C23	0.0875 (8)	0.2800 (9)	0.5114 (4)	4.2 (2)
C24	0.7753 (8)	0.703 (1)	0.4716 (4)	4.7 (2)
C25	0.7110 (8)	0.623 (1)	0.4127 (4)	4.7 (2)
C26	0.7853 (7)	0.562 (1)	0.3709 (4)	4.1 (2)

[a] Values for anisotropically refined atoms are given in the form of the isotropic equivalent displacement parameter defined as $(4/3)[a^2B(1,1) + b^2B(2,2) + c^2B(3,3) + ab(\cos\gamma)B(1,2) + ac(\cos\beta)B(1,3) + bc(\cos\alpha)B(2,3)]$.

Table III. Fractional Atomic Coordinates for $[VO(SALAHE)]_2$ (**3**)

atom	x	y	z	U,[a] Å^2
V1	0.3161 (1)	0.0763 (3)	0.8473 (2)	0.038
V2	0.1828 (1)	0.0304 (3)	0.08796 (2)	0.041
O2	0.3521 (5)	−0.1727 (13)	0.8103 (7)	0.051
O2	0.2390 (4)	0.2132 (13)	0.8125 (6)	0.042
O3	0.3606 (5)	0.2136 (16)	0.9201 (7)	0.059
O4	0.1389 (5)	0.0104 (15)	0.7533 (7)	0.056
O5	0.2603 (4)	−0.0725 (13)	0.9326 (6)	0.044
O6	0.1499 (5)	0.1525 (14)	0.9605 (7)	0.066
N1	0.3294 (6)	0.1788 (18)	0.7059 (8)	0.043
N2	0.1629 (6)	−0.2681 (18)	0.9060 (9)	0.046
C1	0.3927 (7)	−0.2070 (23)	0.7402 (11)	0.045
C2	0.4264 (7)	−0.3893 (22)	0.7475 (12)	0.052
C3	0.4681 (8)	−0.4269 (24)	0.6799 (15)	0.070
C4	0.4753 (9)	−0.3047 (28)	0.5972 (13)	0.074
C5	0.4414 (8)	−0.1219 (25)	0.5849 (12)	0.063
C6	0.4011 (6)	−0.0739 (23)	0.6597 (10)	0.042
C7	0.3657 (7)	0.1107 (20)	0.6390 (11)	0.042
C8	0.2935 (7)	0.3647 (20)	0.6796 (10)	0.048
C9	0.2321 (6)	0.3186 (21)	0.7146 (10)	0.043
C10	0.0998 (7)	−0.1293 (22)	0.7138 (12)	0.048
C11	0.0671 (7)	−0.0865 (23)	0.6248 (13)	0.056
C12	0.0278 (8)	−0.2295 (29)	0.5828 (11)	0.061
C13	0.0173 (8)	−0.4106 (28)	0.6302 (14)	0.069
C14	0.0504 (8)	−0.4597 (23)	0.7187 (14)	0.057
C15	0.0908 (7)	−0.3226 (21)	0.7646 (11)	0.044
C16	0.1250 (7)	−0.3810 (22)	0.8562 (12)	0.048
C17	0.1985 (7)	−0.3437 (21)	0.9927 (10)	0.045
C18	0.2629 (7)	−0.2857 (19)	0.9723 (10)	0.043

[a] $U = {}^1/_3[\sum_i\sum_j U_{ij}a_i^*a_j^*\mathbf{a}_i\cdot\mathbf{a}_j]$.

(40) Cowley, A. H.; Norman, N. C.; Pakulski, M.; Bricker, D.; Russell, D. H. *J. Am. Chem. Soc.* **1985**, *107*, 8211.
(41) Frenz, B. A. The Enraf-Nonius CAD4-SDP.
(42) Sheldrick, G. M. SHELEX 1986, SHELEX76: Programs for Crystal Structure Determinations.
(43) *International Tables for X-ray Crystallography*; Kynoch Press: Birmingham, England, 1974; Vol. 4.
(44) Bartle, K. D.; Dale, B. J.; Jones, D. W.; Maricic, J. *J. Magn. Reson.* **1973**, *12*, 286.

Table IV. Fractional Atomic Coordinates of the Non-Hydrogen Atoms for $\{[VO(SALAMHP)]_2O\}$ (**4c**)

atom	x	y	z	B,[a] Å^2
V1	0.90313 (3)	0.0096 (1)	−0.07881 (5)	2.78 (2)
V2	0.89766 (3)	0.1462 (1)	0.06496 (5)	2.66 (2)
O1	0.9566 (1)	−0.0027 (5)	−0.0747 (2)	3.43 (9)
O2	0.8520 (1)	−0.0739 (6)	−0.0675 (3)	4.3 (1)
O3	0.8918 (1)	0.1051 (6)	−0.1528 (2)	4.5 (1)
O4	0.9001 (1)	0.2109 (5)	−0.0207 (2)	3.29 (9)
O5	0.9179 (1)	−0.0840 (6)	0.0400 (2)	3.50 (9)
O6	0.8490 (1)	0.2445 (6)	0.0732 (2)	3.72 (9)
O7	0.9308 (1)	0.2640 (6)	0.1127 (2)	3.80 (9)
N1	0.9123 (1)	−0.2760 (6)	−0.0997 (2)	2.45 (9)
N2	0.8862 (1)	−0.0324 (6)	0.1452 (2)	2.7 (1)
C1	0.8308 (2)		−0.2268 (9)	3.3 (1)
C2	0.7908 (2)	−0.219 (1)	−0.0642 (4)	4.4 (2)
C3	0.7678 (2)	−0.380 (1)	−0.0719 (4)	5.0 (2)
C4	0.7832 (2)	−0.548 (1)	−0.0879 (4)	5.1 (2)
C5	0.8228 (2)	−0.556 (1)	−0.0971 (4)	4.3 (2)
C6	0.8466 (2)	−0.3963 (8)	−0.0914 (3)	2.9 (1)
C7	0.8874 (2)	−0.4123 (8)	−0.1028 (3)	2.9 (1)
C8	0.9545 (2)	−0.3130 (8)	−0.1101 (3)	3.0 (1)
C9	0.9573 (2)	−0.270 (1)	−0.1857 (3)	4.7 (2)
C10	0.9689 (2)	−0.5130 (9)	−0.0903 (4)	4.5 (2)
C11	0.9780 (2)	−0.1711 (8)	−0.0615 (3)	3.3 (1)
C12	0.8288 (2)	0.2725 (9)	0.1261 (3)	3.1 (1)
C13	0.8007 (2)	0.414 (1)	0.1212 (4)	4.2 (2)
C14	0.7801 (2)	0.446 (1)	0.1778 (4)	5.0 (2)
C15	0.7868 (2)	0.332 (1)	0.2366 (4)	5.4 (2)
C16	0.8136 (2)	0.184 (1)	0.2393 (3)	4.8 (2)
C17	0.8357 (2)	0.1561 (9)	0.1844 (3)	3.4 (1)
C18	0.8622 (2)	−0.0017 (9)	0.1888 (3)	3.2 (1)
C19	0.9114 (2)	−0.2043 (8)	0.1514 (3)	3.3 (1)
C20	0.8932 (2)	−0.3655 (9)	0.1881 (3)	4.6 (2)
C21	0.9538 (2)	−0.155 (1)	0.1879 (4)	1.7 (2)
C22	0.9107 (2)	−0.2529 (8)	0.0742 (3)	3.6 (1)

[a] Values for anisotropically refined atoms are given in the form of the isotropic equivalent displacement parameter defined as $(4/3)[a^2B(1,1) + b^2B(2,2) + c^2B(3,3) + ab(\cos\gamma)B(1,2) + ac(\cos\beta)B(1,3) + bc(\cos\alpha)B(2,3)]$.

Table V. Important Bond Lengths (Å) and Angles (deg) for $VO(HSALAHE)_2$ (**1**)

V1–O1	1.596 (5)	V1–O2	1.904 (5)
V1–O4	1.892 (5)	V1–N1	2.112 (5)
V1–N2	2.097 (5)	V1-oop[a]	0.545 (1)
O1–V1–O2	111.8 (2)	O1–V1–O4	112.8 (3)
O1–V1–N1	100.5 (2)	O1–V1–N1	99.7 (2)
O2–V1–O4	135.4 (2)	O2–V1–N1	86.5 (2)
O2–V1–N2	86.9 (2)	O4–V1–N1	84.4 (2)
O4–V1–N2	86.8 (2)	N1–V1–N2	159.7 (2)

[a] The vanadium out-of-plane (oop) distance toward O1 for the plane defined as O4–O2–N1–N2.

Results and Discussion

Structural Description of Compounds 1, 3, and 4c. $V^{IV}O(HL)_2$ (1). Mononuclear complexes of the type VOL_2 can be prepared in methanol by using $VO(acac)_2$ as the vanadium source and a 2:1 ligand to metal ratio. These compounds are typical five-coordinate, square-pyramidal vanadyl complexes as demonstrated by a variety of physical techniques, including X-ray crystallography. An ORTEP diagram of **1** is provided as Figure 2. Selected bond length and angles are shown in Table V. Each $HSALAHP^-$ is a bidentate, monoanionic ligand, which results in a neutral vanadyl complex. The two HSALAHP ligands are oriented in a trans configuration and use imine nitrogen and phenolate oxygen atoms to bind vanadium. The hydroxyl group is protonated and uncoordinated. The $V–O_{phenolate}$ bonds average 1.898 (5) Å, and the $V–N_{imine}$ bonds average 2.104 (5) Å. These values are in the range seen for many other vanadium Schiff base complexes. The short V–O bond length of 1.596 (5) Å is typical of five-coordinate vanadyl species. The vanadium atom is displaced toward the vanadyl oxygen by 0.545 Å from the best least-squares plane defined by N2, N1, O2, and O4. The other bond lengths and angles are unexceptional. The complex is soluble in DMF, DMSO, and methylene chloride. The change in color of **1** in aerobic solution from green to brown indicates a rapid oxidation to a V(V) complex.

$[V^{IV}O(L)]_2$ (3). Small quantities of a crystalline red complex, **3**, can be isolated when a 1:1 ligand to metal ratio is used and

Table VI. Important Bond Lengths (Å) and Angles (deg) for $[VO(SALAHE)]_2$ (**3**)

V1–O1	1.892 (10)	V1–O2	1.985 (10)
V1–O3	1.619 (10)	V1–O5	1.980 (9)
V1–N1	2.009 (11)	V2–O2	1.979 (9)
V2–O4	1.888 (10)	V2–O5	1.963 (10)
V2–O6	1.548 (9)	V2–N2	2.034 (11)
V1–V2	3.068 (4)		
V2–V1–O1	112.8 (3)	V1–V2–N2	110.1 (4)
V2–V1–O2	39.2 (2)	V1–V2–O2	39.4 (3)
O1–V1–O2	135.2 (4)	V1–V2–O4	110.9 (3)
V2–V1–O3	123.6 (4)	O2–V2–O4	88.2 (4)
O1–V1–O3	111.5 (5)	V1–V2–O5	39.1 (2)
O2–V1–O3	113.2 (5)	O2–V2–O5	77.7 (4)
V2–V1–O5	38.7 (3)	O4–V2–O5	134.6 (4)
O1–V1–O5	91.0 (4)	V1–V2–O6	123.5 (4)
O2–V1–O5	77.1 (4)	O2–V2–O6	109.6 (4)
O3–V1–O5	109.3 (4)	O4–V2–O6	112.9 (5)
V2–V1–N1	110.8 (4)	O5–V2–O6	112.5 (5)
O1–V1–N1	87.8 (4)	O2–V2–N2	143.7 (4)
O2–V1–N1	79.0 (4)	O4–V2–N2	88.4 (5)
O3–V1–N1	104.0 (5)	O5–V2–N2	79.2 (4)
O5–V1–N1	144.6 (4)	O6–V2–N2	105.0 (5)

Table VII. Important Bond Lengths (Å) and Angles (deg) for $\{[VO(SALAMHP)]_2O\}$ (**4c**)

V1–O1	1.805 (4)	V1–O2	1.880 (4)
V1–O3	1.598 (4)	V1–O4	1.857 (4)
V1–O5	2.404 (4)	V1–N1	2.130 (5)
V2–O4	1.759 (4)	V2–O5	1.828 (4)
V2–O6	1.888 (4)	V2–O7	1.591 (4)
V2–N2	2.115 (5)	V1–V2	3.06
O1–V1–O2	156.5 (2)	O1–V1–O3	99.2 (2)
O1–V1–O4	99.3 (2)	O1–V1–O5	83.5 (2)
O1–V1–N1	77.6 (2)	O2–V1–O3	98.6 (2)
O2–V1–O4	92.2 (2)	O2–V1–O5	81.5 (2)
O2–V1–N1	83.0 (2)	O3–V1–O4	101.1 (2)
O3–V1–O5	170.4 (2)	O3–V1–N1	105.2 (2)
O4–V1–O5	69.3 (1)	O4–V1–N1	153.7 (2)
O5–V1–N1	84.3 (2)	V1–O5–V2	88.6 (1)
O4–V2–O5	84.9 (2)	O4–V2–O6	99.2 (2)
O4–V2–O7	106.7 (2)	O4–V2–N2	156.1 (2)
O5–V2–O6	137.2 (2)	O5–V2–O7	111.7 (2)
O5–V2–N2	77.0 (2)	O6–V2–O7	107.8 (2)
O6–V2–N2	84.0 (2)	O7–V2–N2	94.6 (2)

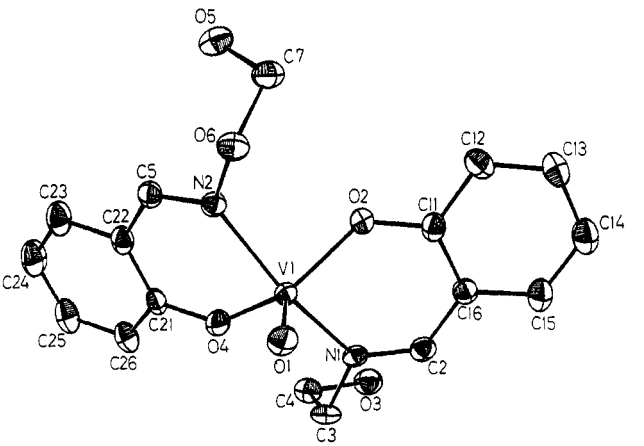

Figure 2. ORTEP diagram of $VO(HSALAHE)_2$ (**1**) with thermal ellipsoids at 30% probability, showing the atom-labeling scheme.

(45) Evans, D. F. *J. Chem. Soc.* **1959**, 2003.

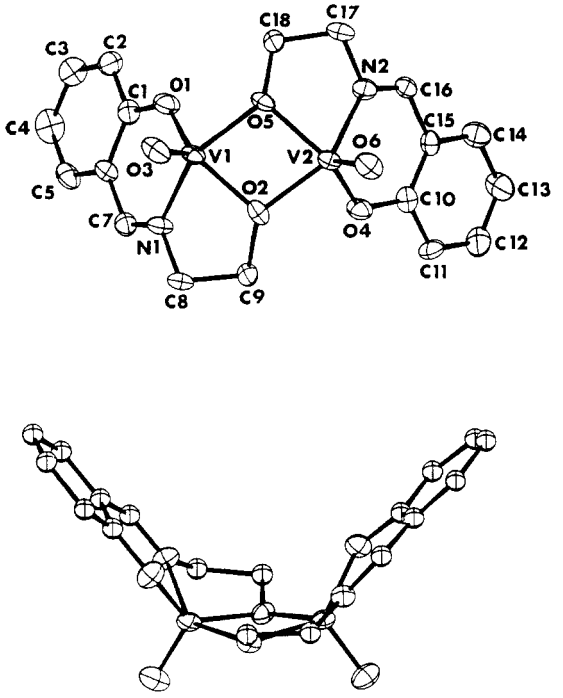

Figure 3. ORTEP diagram of $[VO(SALAHE)]_2$ (**3**) with thermal ellipsoids at 30% probability. The upper view contains the atom-labeling scheme, while the lower view shows the highly bent nature of the molecule.

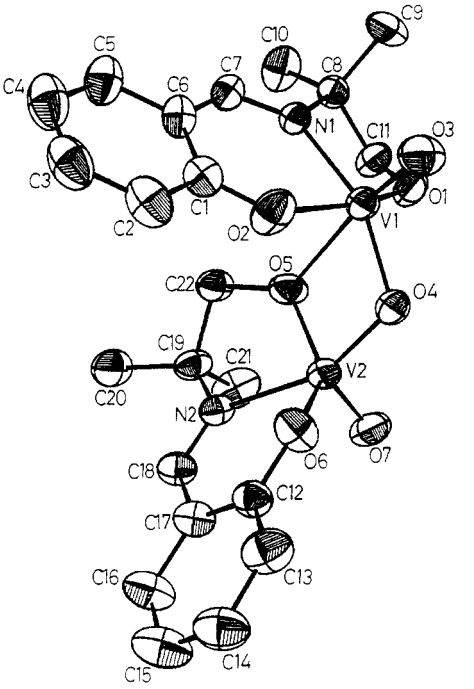

Figure 4. ORTEP diagram of $\{[VO(SALAMHP)]_2O\}$ (**4c**) with thermal ellipsoids at 30% probability, showing the atom-labeling scheme.

precautions to exclude oxygen are taken. This paramagnetic material analyzes for VOL. Solid-state magnetic measurements gave a room-temperature magnetic moment of $\mu_{eff} = 1.52$ (5) μ_B per vanadium suggesting weak antiferromagnetic coupling between the V(IV) atoms. A dimeric formulation was confirmed by X-ray crystallography, which showed two VOL units linked by alkoxide bridges as illustrated in Figure 3. Bond lengths and angles for **3** are tabulated in Table VI.

While the $V-O_{phenolate}$ distances, which average 1.89 Å, are practically identical with those found in the mononuclear complex **1**, the $V-N_{imine}$ distances of 2.02 Å in **3** are almost 0.1 Å shorter. This is a result of the meridional, tridentate coordination adopted by the $SALAHE^{2-}$ ligand, which, due to the contiguous five- and six-membered chelate rings, requires a more compressed nitrogen distance. The strain involved in coordinating the alkoxide oxygen in **3** leads to a much less regular polyhedron than that around the vanadium in **1**. Although the vanadyl oxygen bonds average nearly the same as those seen in **1** (1.58 Å), the absolute values between the two vanadiums in **3** differ substantially, ranging between that for V1–O3 (1.619 Å) and that for V2–O6 (1.548 Å). We have no explanation for these differences at present although this 0.07-Å difference is presumably significant since it is 7 times the esd's. The bridging vanadium alkoxo oxygen bonds average 1.976 Å (range 1.985–1.963 Å) with the bonds to V2 slightly shorter than those to V1 although this is the doubtful significance. The V1–O5–V2 and V1–O2–V2 angles of 102.2 and 101.3°, respectively, lead to a V–V distance of 3.068 Å.

The meridional, tridentate chelation of the SALA series of ligands has been well documented in manganese chemistry for mononuclear,[46-48] dinuclear,[49,50] and trinuclear complexes.[51,52] Of specific interest here are the dialkoxy-bridged dimers $[Mn^{III}(SALAHP)(OAc)]_2$[49] (Mn–Mn = 2.869 Å) and $[Mn^{III}(SALAHP)(CH_3OH)Cl]_2$[50] (Mn–Mn = 3.011 Å). In both cases, the four-atom $[Mn(OR)]_2$ core is strictly planar, and in the chloro adduct, the trans isomer is isolated exclusively. This is in marked contrast to **3** where the four-atom $[V(OR)]_2$ core is bent and the two vanadyl groups are in a "syn" configuration. A recent structure determination[53] of the dialkoxy-bridged dimer $[(\mu\text{-}\eta^3\text{-}C_5Me_5O_3)V(O)]_2$ showed that the terminal oxo groups of the V(V) ions in this complex were also arranged in a syn configuration. Previous workers[31-37] have suggested that the green-gray isomer **2** formed a spin ladder with a planar core and an anti orientation of the vanadyl oxygen atoms. The impact of these two orientations of the terminal oxygen atoms on magnetochemistry of this system will be discussed below.

$[V^VOL]_2$ (4c). As illustrated in Figure 4, **4c** crystallizes as a highly asymmetric oxo-bridged V(V/V) dimer with V1 adopting a distorted six-coordinate octahedral geometry while V2 adopts a five-coordinate square-pyramidal structure. The V1 coordination sphere is composed of a phenolate oxygen (V1–O2 = 1.88 Å), an imino nitrogen (V1–N1 = 2.12 Å) and a deprotonated alkoxide oxygen (V1–O1 = 1.805 Å) from the Schiff base ligand, a terminal oxo group (V1–O3 = 1.598 Å), and a second oxo atom (V1–O4 = 1.857 Å) that forms a strong bridge to V2 (V2–O4 = 1.759 Å). A second, weaker bridge between V1 and V2 is formed by the alkoxide oxygen of the ligand coordinated to V2 (Table VII). The V2–O5 distance is 1.888 Å as compared to the V1–O5 bond, which is 2.404 Å. The remainder of the V2 coordination sphere is filled by phenolate oxygen (V2–O6 = 1.828 Å) and imine nitrogen (V2–N2 = 2.115 Å) atoms of the ligand, as well as a terminal oxo group (O7) at 1.591 Å.

Although the SALAMHE ligand cannot adopt a facial orientation it does distort from its normal meridional orientation (O5–V2–O6 = 137.2° vs O1–V1–O2 = 156.5°) in order to allow the weak association between V1 and O5 to occur. However, while this ligand deviation from meridional geometry can block the sixth coordination site from solvent, it alone is not sufficiently large to allow coordination of O5 to V1 and the V2(O)L unit must twist

(46) Kessissoglou, D. P.; Butler, W. M.; Pecoraro, V. L. *J. Chem. Soc., Chem. Commun.* **1986**, 1253.
(47) Kessissoglou, D. P.; Li, X.; Butler, W. M.; Pecoraro, V. L. *Inorg. Chem.* **1987**, *26*, 2487.
(48) Li, X.; Lah, M. S.; Pecoraro, V. L. *Acta Crystallogr., Sect. C* **1989**, *45*, 1517.
(49) Mikuriya, M.; Torihara, N.; Okawa, H.; Kida, S. *Bull. Chem. Soc. Jpn.* **1981**, 1063.
(50) Li, X.; Larson, E.; Bonadies, J. A.; Lah, M. S.; Armstrong, W. A.; Pecoraro, V. L. Submitted for publication in *Inorg. Chem.*
(51) Li, X.; Kessissoglou, D. P.; Kirk, M. L.; Bender, C. J.; Pecoraro, V. L. *Inorg. Chem.* **1988**, *27*, 1.
(52) Kessissoglou, D. P.; Bender, C.; Kirk, M. L.; Lah, M. S.; Pecoraro, V. L. *J. Chem. Soc., Chem. Commun.* **1989**, 84.
(53) Bottomley, F.; Magill, C. P.; White, P. S. *J. Am. Chem. Soc.* **1989**, *111*, 3070.

away from a syn orientation of terminal oxygen atoms resulting in a V1–O3···V2–O7 torsion angle of ≈105°. Finally, the V1–O4–V2 bond angle of 113° is well short of linear due to the coordination of the bridging alkoxide.

A comparison of analogous bond lengths between V1 and V2 reveals some interesting differences. The oxo bridge is asymmetrically disposed between the two vanadium centers with the pentacoordinate V2 having a 0.1 Å shorter V–O_{oxo} bridge than the hexacoordinate V1. The bridging alkoxide is also asymmetrically disposed with the very long V1–O5 bond length of 2.4 Å attributable to the fact that O5 is trans to the terminal oxo group. The magnitude of this trans effect is well within the range seen in other mono- and dioxovanadium(V) complexes.

At first glance, the isolated structure may seem to have little order; however, a consideration of the ligand charge, steric constaints, the oxophilicity/electron deficiency of V(V), and strong π donor properties of terminal oxo groups can be combined to explain the recovered product. It is apparent that the majority of structurally characterized Mn and V Schiff base complexes, especially of the SALA series, are of the neutral complexes. All of the tridentate SALA ligands are dianions. Thus, a neutral species is formed by the addition of three negative charges. Two can be supplied by a terminal oxo group. A second terminal oxo would have resulted in the monoanion $[VO_2L]^-$. Instead, dimerization to form the vanadate anhydride, with a bridging oxo, provides overall charge neutrality. Recently, we have reported[13] dimers of formulation $[VO_2L]_2$ where L = SHED. In this case, the SHED ligand is a monoanion that donated neutral imine and amine nitrogens and a phenolate oxygen; therefore, inclusion of two oxo groups resulted in the neutral vanadium complex. Both the SALA and SHED ligands have a strong preference for meridional coordination. Examination of the V1 and V2 coordination spheres illustrates that this basic preference has been maintained, although a significant deviation is seen in the ligand coordinated to V2. Such meridional isomers are well suited to the formation of *cis*-pervanadyl units $[VO_2^+]$. These terminal oxo groups are oriented cis due to the strong π character of the V=O bonds. The dimerization of VO_2(SHED) units is driven by the electron de-

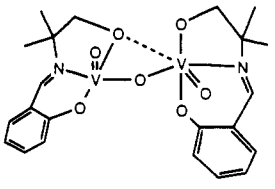

$[V(SALAMHP)O]_2O$

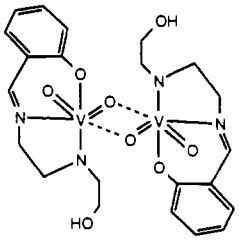

$[VO_2(SHED)]_2$

ficiency and oxophilicity of the V(V) ion. The structure of **4c** is similarly influenced by this electron deficiency as the alkoxide oxygen (O5) donates an electron pair to V1 leading directly to the nonlinear μ-oxo bridge. This is in contrast to what happens with a structurally similar tridentate, dianionic O_2N ligand reported by Diamantis et al., where the dimeric V(V) complex has a strictly linear oxo bridge with no secondary bridging interactions.[54] We believe the differences between the two structures can be accounted for by the much higher basicity of the alkoxy group in **4c** as compared with the 2,4-dione in the Diamantis complex.

Solid-State Magnetochemistry of 2 and 3. Dimeric d^1 V(IV) complexes represent interesting compounds for the study of spin-exchange phenomena. The spin-only moment for isolated V(IV) ions is 1.73 μ_B. This value can be reduced due to spin–orbit coupling, designated by λ, or by exchange coupling between two metal centers of a dimer. Fortunately, spin–orbit coupling in nearly all V(IV) complexes is efficiently quenched so that reduction of the magnetic moment usually indicates a mechanism for antiferromagnetic coupling between the vanadium centers.[55] Unlike the related d^9 Cu(II) systems, which have $d_{x^2-y^2}$ as the magnetic orbital, the magnetic orbital in square-pyramidal V(IV), as determined by EPR spectroscopy,[56] is the d_{xy}. An excellent pathway for superchange in Cu(II) dimers results because the $d_{x^2-y^2}$ orbital points toward the bridging ligand groups. In contrast, the orbitals on two adjacent V(IV) ions are aligned and can, in principle, lead to direct σ overlap, resulting in a decreased magnetic moment. Indeed, this mechanism has been invoked as the primary path for magnetic coupling in bis(μ-alkoxo)- and bis(μ-phenolato)vanadium(IV) complexes.[57] Alternative pathways such as superexchange via $d_{x^2-y^2}$ through excited-state mixing of d_{xy} and $d_{x^2-y^2}$ is thought to be negligible.

Dimeric complexes of V(IV) with *N*-(hydroxyalkyl)-salicylideneamine ligands have been reported previously by a number of authors,[31-37] but the literature remains controversial due to the lack of accurate structural information. Compound **3** represents the first structurally characterized member of this class of complexes and allows us to put the magnetochemistry on a firmer footing. The structure of **3** clearly reveals the alkoxy-bridged dimeric formulation previously suggested for these complexes. However the vanadyl oxygens adopt the "syn" rather than the expected "anti" configuration. Although we have not done a complete temperature-dependent magnetic study (this will be reported in due course) and hence cannot determine the exchange-coupling constant, $-2J$, the magnitude of the room-temperature moment indicates that the degree of exchange coupling in **3** is less than that seen in an analogous "syn" hydroxy-bridged dimer, $[V_2O_2(\mu\text{-}OH)_2(tpen)]^{2+}$[58] but is similar to the presumed phenoxy-bridged complexes reported by Ginsberg.[57]

A second polynuclear complex **2**, with the same analytical formulation as **3** has also been characterized. The very low magnetic moment for **2** (1.01 (5) μ_B) indicates that the vanadium atoms are even more strongly coupled than in **3** (1.52 (5) μ_B). Solid-state magnetic measurements on **2** have also been reported on Yamada et al. as 1.09 μ_B,[37] by Poddar et al. as 1.41 μ_B,[32] and by Syamal as 0.89–1.41 μ_B.[55] Our value of 1.01 μ_B for **2** agrees closely with that of Yamada's group and it seems likely that the complex reported by Theriot and Syamal is either the red isomer or a mixture of **2** and **3**.

Two structural organizations could account for the moment reduction seen in **2**. If **2** is the "anti" isomer of **3**, it is likely that this compound will align the d_{xy} orbitals on each V(IV) ion in a position better for σ overlap than would be the case for the bent complex **3**. Thus, the observed reduction in moment is consistent with the through-space model of Ginsberg et al.[57] Futhermore, this mechanism would explain why the exchange coupling for a well-characterized set of syn and anti hydroxo-bridged V(IV) dimers prepared by Wieghardt et al.[58] are of a similar magnitude. For these complexes, both the syn and anti configurations have planar or nearly planar

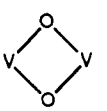

rings. Thus there is predicted to be little difference in the degree of direct σ overlap of the d_{xy} orbitals.

Although the Ginsberg model successfully describes both our and Wieghardt's dimers, an alternative structure that cannot be ruled out by the magnetic behavior would be an infinite spin ladder formulation for **2** (Figure 5), which has been proposed previously.[37] However, Hatfield has studied the exchange interaction in VO(SALEN) infinite chains,[59] which model the d_{z^2} superexchange

(54) Diamantis, A. A.; Fredensken, J. M.; Salam, M. A.; Snow, M. R.; Tiekink, R. T. *Aust. J. Chem.* **1986**, *39*, 1081.

(55) Syamal, A. *Coord. Chem. Rev.* **1975**, *16*, 309.
(56) Selbin, J. *Coord. Chem. Rev.* **1966**, *1*, 293.
(57) Ginsberg, A. P.; Koubek, E.; Williams, H. J. *Inorg. Chem.* **1966**, *5*, 1656.
(58) Neves, A.; Wieghardt, K.; Nuber, B.; Weiss, J. *Inorg. Chim. Acta* **1988**, *150*, 183.

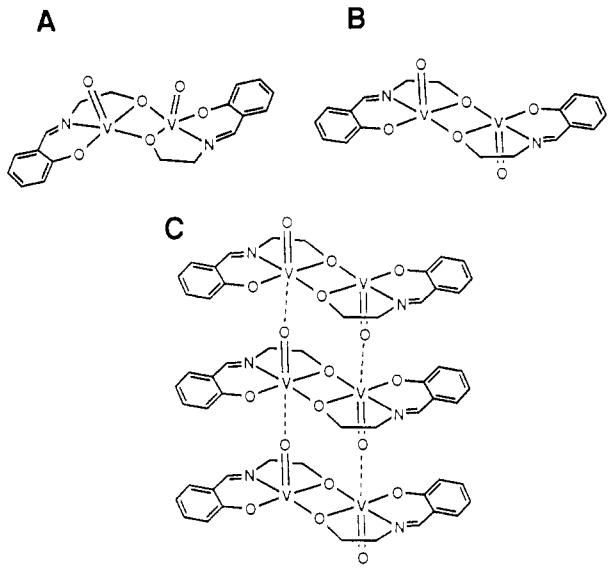

Figure 5. Structures of V(IV) complexes in (A) syn, (B) anti, and (C) anti-"spin-ladder" forms.

Table VIII. ^{13}C NMR Spectral Data for V(V) Dimers

complex	^{13}C	$\delta_{complex}$	δ_{ligand}	$\Delta\delta$
4a	a	164.6	162.0	+2.6
	b–f	136.3	132.2	+4.1
		134.2	131.2	+3.0
		120.1	117.9	+2.2
		119.4	117.6	+1.8
		118.1	116.8	+1.3
	g	164.7	166.0	−1.3
	i	66.2	60.1	+6.1
	j	75.2	60.9	+14.3
4c	a	163.1	162.2	+0.9
	b–f	135.7	132.4	+3.3
		133.3	131.3	+2.0
		119.6	118.0	+1.6
		119.2	117.9	+1.3
		117.1	117.1	+0.0
	g	163.9	166.2	−2.3
	i	88.0	66.5	+15.5
	j	73.1	65.5	+7.6
	h	20.3	20.4	+0.1
4d	a	162.0	161.7	+0.3
	b–f	135.8	132.9	+2.9
		133.8	131.7	+2.1
		120.3	118.1	+2.2
		119.2	117.4	+2.0
		116.8	116.5	+0.3
	g	162.7	165.4	−2.7
	i	87.8	69.3	+18.5
	j	75.0	59.7	+15.3
	h, h′	25.3	22.9	+2.4

pathway of the spin ladder, and found a ferromagnetic exchange constant only on the order of $J = +4.2$ cm^{-1}. Nevertheless, without further structural data, we cannot distinguish the discrete anti dimer from the infinite spin ladder.

Solution Interconversion of Complexes. Under conditions of excess ligand, V(IV) complexes of the *N*-(hydroxyalkyl)-salicylideneamines exist as discrete mononuclear complexes and adopt the five-coordinate square-pyramidal geometry so often seen with the VO^{2+} center. The green VO(SALAHE)$_2$ (**1**) undergoes slow air oxidation in alcohols or DMF; however, when **1** is dissolved in nonpolar solvents such as CH_2Cl_2, it converts rapidly to the asymmetric V(V/V) dimer **4**. This dimer can also be formed from the V(IV/IV) dimers **2** or **3** if dioxygen is admitted to the reaction vessel. The oxidation of **2** probably proceeds through monomeric

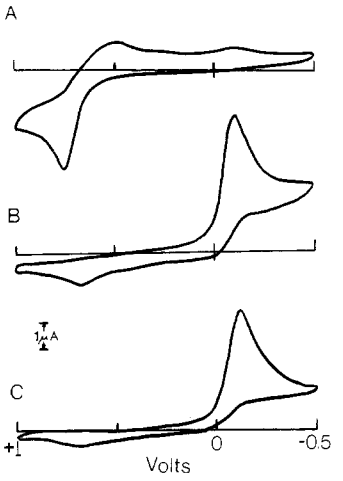

Figure 6. Cyclic voltammograms: (A) **3** in acetonitrile (scan rate = 100 mV/s); (B) Solution from part A after exposure to air for 1 day; (C) **4a** in acetonitrile (scan rate = 100 mV/s).

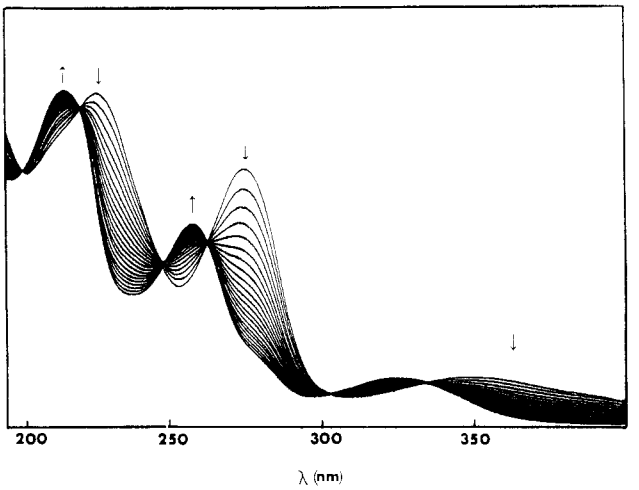

Figure 7. UV spectral changes accompanying hydrolysis of **4c** in neutral aqueous solution (scan time 480 nm/min, 2 min between successive scans).

intermediates since solutions in DMF of CH_2Cl_2 are ESR active and have a solution moment of 1.73 (5) μ_B. These observations suggest that the spin coupling seen in the solid state is broken in solution, yielding discrete mononuclear V(IV) species.

The route by which **3** is converted into **4a** deserves some comment since, on the basis of their respective structures, it is clear that the V(IV) dimer cannot be converted to the V(V) dimer by a simple outer-sphere oxidation. In contrast to **2**, solutions of **3** are EPR silent, providing that **3** does not dissociate into monomeric units. Similarly, the proton and ^{13}C NMR spectra of **4a**, tabulated in Table VIII, confirms the alkoxy group is deprotonated and coordinated to the V(V) center. Analysis of the ^{13}C NMR spectra in particular show that most of the resonances are within 0–3 ppm of those of the free ligand except those assigned to carbons α and β to the alcohol oxygen. These carbon resonances are shifted some 8–20 ppm downfield of the analogous resonance in the free ligand with the α-carbon experiencing the greater shift. The cyclic voltammogram of **3** in acetonitrile (Figure 6A) shows an irreversible oxidation at +746 mV vs SCE with a product reduction at −110 mV. Similar electrochemistry, with no scan rate dependence (50–1000 mV/s), is observed in all solvents tested. A reduction at −112 mV with a product oxidation at +690 mV is found when the cyclic voltammogram of **4a** is obtained in acetonitrile (Figure 6B). When **3** is bulk oxidized at +850 mV, >1.8 electrons per dimer are passed and the cyclic voltammogram of **4a** is obtained. The process is chemically reversible as this solution may be electrolyzed at 0 V resulting in the cyclic voltammogram of **3**. Identical chemistry is found when authentic samples of **4a** are the starting point for the electrolysis. There were no EPR-

(59) Drake, R. F.; Crawford, V. H.; Hatfield, W. E.; Simpson, G. C.; Carlisle, G. O. *J. Inorg. Nucl. Chem.* **1975**, *37*, 291.

detectable species when the electrolysis of **3** was stopped at 50% completion, which rules out an appreciable concentration of V(IV) monomer, which should give an 9-line spectrum, or a mixed-valence dimer, which should have a multiline (≥17-line) spectrum. These data indicate that **3** and **4a** interconvert without the presence of detectable intermediates on the CV time scale.

Although the V(V) complexes prepared appear to be quite robust with respect to internal redox reactions, they are hydrolytically unstable. Dissolution of complexes in neutral aqueous solution leads to a series of UV spectral changes (Figure 7) that can be interpreted as hydrolysis of the Schiff base ligand. The alternative explanation (i.e. that water promotes the dissociation of the dimer) appears unlikely since the spectral changes seen are virtually the same as those when the ligand itself undergoes hydrolysis in aqueous solution.

In summary, the hydroxyl-rich Schiff base ligands described herein are unable to satisfy completely the coordination number of higher valent vanadium. Rather than obtaining discrete mononuclear pervanadyl compounds, one recovers stable dimers in the +4 and +5 oxidation states. The interconversion of these dimeric materials suggests that small quantities of mononuclear V(V) compounds may be accessible, especially in polar solvents. However, the instability of the imine linkage in water must be considered in future synthetic design. Fortunately we have been able to prepare stable, mononuclear peroxyvanadium(V)-SALA complexes as deep red solids. It is these compounds that we believe can be used to evaluate possible mechanistic proposals for the catalytic bromination of olefins by the vanadium bromoperoxidase.

Acknowledgment. We wish to thank Erlund Larson and Myoung Soo Lah for very useful technical assistance and discussions. V.L.P. thanks the G. D. Searle Family/Chicago Community Trust for a Biomedical Research Scholar's Award (1986-1989) and The Alfred P. Sloan Foundation for a Sloan Fellowship (1989-1991). C.J.C. acknowledges the support of the Robert A. Welch Foundation and thanks Professors Alan Cowley and Richard Jones, University of Texas at Austin, for the generous use of their X-ray diffractometer.

Supplementary Material Available: Table 9 (electrochemical potentials), Tables 10-12 (anisotropic thermal parameters), Table 13 (fractional atomic coordinates for hydrogen atoms in **3**), Tables 14-19 (complete bond angles and bond distances), and Table 23 (complete crystallographic data) (14 pages); Tables 20-22 (observed and calculated structure factors) (32 pages). Ordering information is given on any current masthead page.

Contribution from the Département de Chimie, Université de Montréal, Montréal, Québec, H3C 3J7 Canada

Coordination Chemistry of Zirconium Tetrachloride. Crystal Structure of the 1:2 Adduct with Pinacolone

Bruno Galeffi, Michel Simard, and James D. Wuest*

Received June 26, 1989

Studies of adducts **1-4** of zirconium tetrachloride with acetone, pinacolone, 3-pentanone, and tetrahydrofuran by infrared spectroscopy in solution and in the solid state, and by low-temperature ^{1}H NMR spectroscopy in solution, suggest that all four bases form octahedral 1:2 complexes. This conclusion is supported by the results of an X-ray crystallographic study of the 1:2 pinacolone adduct **2**, which crystallizes in the orthorhombic space group $P2_12_12_1$ with a = 9.660 (3) Å, b = 11.935 (4) Å, c = 16.813 (7) Å, V = 1938.4 Å^3, and Z = 4. Refinement of 3259 reflections yielded R = 0.18. The structure shows that the ketones are cis and σ-bound with an average C-O-Zr angle of 151°. In solution, bound and free acetone exchange by dissociation of complex **1** with $\Delta G^{\ddagger}$ = 12.4 kcal/mol. Syn-anti isomerization is rapid in acetone adduct **1** and 3-pentanone adduct **3** even at -120 °C in CHF_2Cl, possibly because significant oxygen-p-zirconium-d π-bonding or an important electrostatic contribution to the energy of complexation facilitates inversion at oxygen.

Zirconium tetrachloride forms adducts with a wide variety of Lewis bases,[1] but no detailed structural information about these complexes is available.[2,3] In this paper, we characterize representative 1:2 adducts of zirconium tetrachloride with acetone (**1**),[4]

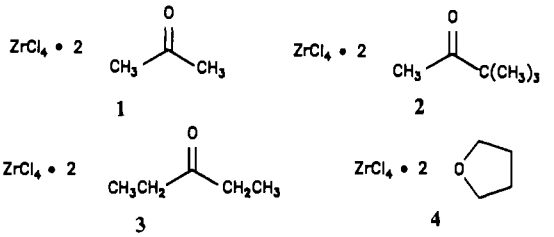

pinacolone (**2**), 3-pentanone (**3**), and tetrahydrofuran (**4**)[5] by infrared spectroscopy in solution and in the solid state and by low-temperature ^{1}H NMR studies in solution. In addition, we describe the crystal structure of the pinacolone adduct **2**.

Treatment of a suspension of zirconium tetrachloride in dichloromethane at 0 °C with 2 equiv of acetone produced an adduct that crystallized in 79% yield after partial evaporation of the solvent. Earlier elemental analyses had already established the 1:2 stoichiometry of the product.[4a,b] The presence in its infrared spectrum of shifted carbonyl stretching bands at 1660 and 1635 cm^{-1} (Nujol) and at 1665 cm^{-1} ($CHCl_3$) confirmed that both

(1) Fay, R. C. In *Comprehensive Coordination Chemistry*; Wilkinson, G., Gillard, R. D., McCleverty, J. A., Eds.; Pergamon: Oxford, England, 1987; Vol. 3, pp 363-451.

(2) For recent references to structural studies of related adducts of titanium chlorides, see: (a) Oppolzer, W.; Rodriguez, I.; Blagg, J.; Bernardinelli, G. *Helv. Chim. Acta* **1989**, *72*, 123-130. (b) Maier, G.; Seipp, U.; Boese, R. *Tetrahedron Lett.* **1987**, *28*, 4515-4516. (c) Utko, J.; Sobota, P.; Lis, T. *J. Organomet. Chem.* **1987**, *334*, 341-345. (d) Reetz, M. T.; Hüllman, M.; Seitz, T. *Angew. Chem., Int. Ed. Engl.* **1987**, *26*, 477-479. (e) Keck, G. E.; Castellino, S. *J. Am. Chem. Soc.* **1986**, *108*, 3847-3849. (f) Poll, T.; Metter, J. O.; Helmchen, G. *Angew. Chem., Int. Ed. Engl.* **1985**, *24*, 112-114. (g) Bassi, I. W.; Calcaterra, M.; Intrito, R. *J. Organomet. Chem.* **1977**, *127*, 305-313.

(3) For recent references to structural studies of related adducts of $SnCl_4$, see: (a) Reetz, M. T.; Harms, K.; Reif, W. *Tetrahedron Lett.* **1988**, *29*, 5881-5884. (b) Denmark, S. E.; Menke, B. R.; Weber, E. *J. Am. Chem. Soc.* **1987**, *109*, 2512-2514. (c) Keck, G. E.; Castellino, S. *Tetrahedron Lett.* **1987**, *28*, 281-284. (d) Lewis, F. D.; Oxman, J. D.; Huffman, J. C. *Ibid.* **1984**, *106*, 466-468.

(4) (a) Graven, W. M.; Peterson, R. V. *J. Inorg. Nucl. Chem.* **1969**, *31*, 1743-1748. (b) Paul, R. C.; Chadha, S. L. *Ibid.* **1969**, *31*, 1679-1683. (c) Osipov, O. A.; Kletenik, Yu. B. *Zh. Obshchei Khim.* **1961**, *31*, 2451-2456. (d) Joseph, P. T.; Blumenthal, W. B. *J. Org. Chem.* **1959**, *24*, 1371-1372.

(5) (a) Manzer, L. E. *Inorg. Synth.* **1982**, *21*, 136. (b) Westland, A. D.; Uzelac, V. *Can. J. Chem.* **1970**, *48*, 2871-2876. Chung, F. M.; Westland, A. D. *Ibid.* **1969**, *47*, 195-199.

0020-1669/90/1329-0951$02.50/0